

# Size Exclusion Chromatography with Dual Wavelength Detection as a Sensitive and Accurate Method for Determining the Empty and Full Capsids of Recombinant Adeno-Associated Viral Vectors

He Meng<sup>\*1</sup>, Michelle Sorrentino<sup>1</sup>, Denise Woodcock<sup>2</sup>, Catherine O’Riordan<sup>2</sup>, Vijender Dhawan<sup>1</sup>, Marc Verhagen<sup>1</sup>, and Claire Davies<sup>1</sup>

1. BioAnalytics, Global CMC Development, Sanofi, Framingham, Massachusetts, 01701, USA
2. Gene Therapy Research, Sanofi, Framingham, Massachusetts, 01701, USA

Running Title: SEC-DW for Empty and Full Capsids of AAVs

\*Corresponding author:

*Dr. He Meng, BioAnalytics, Global CMC Development, Sanofi, 5 The Mountain Road, Framingham, MA 01701.*

*E-mail: he.meng@sanofi.com*

*Phone: +1 508 661 1792*

Keywords: AAV, AUC, Cryo-EM, empty and full capsids, gene therapy, and SEC-DW

Abstract Word count: (313)

## Abstract

Gene therapy has evolved over the past decade into a promising therapeutic class for treating many intractable diseases. Recombinant adeno-associated virus (AAV) is the most commonly used viral vector for delivering therapeutic genes. Independent of the manufacturing process for AAVs, the clinical materials are inherently heterogeneous and contain both empty and full capsids. Empty capsids can impact the safety and efficacy of AAV products and therefore their level needs to be controlled. Several analytical methods have been reported for this purpose. However, some of these methods have an insufficient assay range, or rely on instruments that cannot be readily implemented in a QC environment. Here, we describe a fast size exclusion chromatography (SEC) assay with dual-wavelength detection (SEC-DW) to directly determine the percent full capsids of AAV samples based on their peak area (PA) ratios. The two detection wavelengths selected to represent encapsidated transgenes and capsid proteins are 260 nm and 230 nm, respectively instead of the conventionally used 260 nm and 280 nm. The use of 230 nm instead of 280 nm to monitor the contribution of the capsid protein results in a linear relationship between the PA<sub>260</sub>/PA<sub>230</sub> ratio and the percent full capsids, unlike the non-linear relationship observed when the PA<sub>260</sub>/PA<sub>280</sub> ratio is used. As a result, the method exhibits a significantly extended assay range (up to 91% full capsids). The accuracy of the SEC-DW method was confirmed by comparing the results obtained against results from orthogonal high-resolution methods such as analytical ultracentrifugation (AUC) and cryo-electron microscopy (Cryo-EM) and excellent agreement was obtained when common samples were analyzed using the different methods. The SEC-DW method runs on a readily accessible HPLC instrument platform, provides much higher assay throughput compared to AUC and electron microscopy (EM), and can be implemented as a release method in a QC environment or used as a rapid screening tool to support process development and product understanding.

**Keywords:** AAV, AUC, Cryo-EM, empty and full capsids, gene therapy, and SEC-DW

## Introduction

Adeno-associated virus (AAV) is a small nonpathogenic parvovirus, in which a linear single stranded DNA genome with a size of approximately 4.7 kilobases is packaged into a nonenveloped icosahedral capsid. The viral genome consists of three viral genes *rep* (replication), *cap* (capsid), and *aap* (assembly-activating protein) flanked by two inverted terminal repeats (ITRs)<sup>1</sup>. The capsid is assembled as a 60-mer from three viral proteins (VPs) VP1, VP2, and VP3 with an approximately 5:5:50 ratio<sup>2</sup>. In therapeutic recombinant AAVs (rAAVs), the viral genome is replaced with a transgene, while the ITRs are retained for proper genome replication and packaging. The transgene is converted into a double stranded DNA for gene expression after entering the target cell nucleus, to exert therapeutic effects.

To date, three rAAV gene therapies have been approved, Glybera for rare lipoprotein lipase deficiency (EMA, 2012); Luxturna for Leber's congenital amaurosis (FDA, 2017) and Zolgensma for spinal muscular atrophy (FDA, 2019)<sup>3</sup>. Many more rAAVs are in clinical trials for various disease indications<sup>3-5</sup>. During manufacturing, vectors harboring full-length genome (full capsids), no genome (empty capsids), fragments of genome (partial capsids), and non-transgene related host cell DNAs are produced<sup>6</sup>. While *bona fide* full capsids are purified as desired product, some empty capsids cannot be easily removed and are inevitably present in the drug substance (DS) due to their similar structural properties<sup>1, 7, 8</sup>. Although the impact of the presence of empty capsids on therapeutic outcomes is not fully understood yet, Gao et al. reported that empty capsids reduced transduction efficiency and induced liver transaminitis in mouse models<sup>9</sup>. In contrast, Mingozi et al. suggested that empty capsids can serve as decoys to mitigate the inhibitory effect of pre-existing anti-AAV antibodies and actually enhance gene transfer efficiency<sup>10, 11</sup>. Independent of the impact of empty capsids<sup>12, 13</sup>, the level of empty capsids needs to be monitored to further our understanding of their impact on safety and efficacy, and controlled to ensure the consistency of product quality<sup>14, 15</sup>.

Multiple methods have been reported for quantifying empty or full capsids in AAVs. Sommer et al. quantified empty capsids in purified AAV samples based on the  $A_{260}/A_{280}$  ratio from optical density measurements after sample denaturation. The capsid-to-vector

genome ratios (cp/vg) correlated well with the ratios determined by qPCR and capsid ELISA<sup>16</sup>. However, since the specificity of the method is limited, non-vector proteins, free nucleic acids, and other components can significantly affect the accuracy of this method. Transmission electron microscopy (TEM) has been used to visualize AAV particles after negative staining<sup>17</sup>. Empty and full capsids are differentiated based on the electron density and counted to yield percent full capsids. Burnham et al. employed analytical ultracentrifugation sedimentation velocity (AUC-SV) experiments to characterize AAV vectors based on their sedimentation behavior in a centrifugal field<sup>18</sup>. In addition to empty, full, and partial capsids, AUC-SV can also resolve higher order species and fragmented capsids. Pierson et al. used charge detection mass spectrometry (CDMS) to determine the distribution of empty, partial and full capsids by concurrently measuring the mass charge ratio ( $m/z$ ) and the charge ( $z$ ) of individual ions<sup>19</sup>. Li et al. has recently introduced a capillary isoelectric focusing (cIEF) method to determine the empty and full ratio of AAV vectors<sup>20</sup>. These methods distinguish the empty and full capsids using different mechanisms, and therefore provide complementary insights in the composition of the sample. However, some methods such as AUC and CDMS are difficult to implement in a quality control (QC) environment, and some may face challenges due to inadequate assay range or low throughput. Chromatographic methods, being high-throughput, as well as readily accessible and deployed in QC and development labs, can therefore be useful for determining the level of empty and/or full capsids.

Anion exchange chromatography (AEX) has been used for determining the level of empty capsids in several serotypes by exploring the minor difference in isoelectric point ( $pI$ ) between empty and full capsids. Lock et al. resolved density gradient purified AAV8 empty capsids from full capsids using a fast flow liquid chromatography instrument equipped with a CIM-QA monolithic disk<sup>21</sup>. Fu et al. separated empty capsids of a nondisclosed serotype and affinity purified AAV over a CIMac AAV full/empty-0.1 analytical column<sup>22</sup>. Wang et al. optimized the separation of empty capsids of an AAV6.2 sample over the CIMac AAV full/empty-0.1 analytical column and employed an empirical response conversion factor to quantitate empty capsids based on the fluorescence signal<sup>23</sup>. Although these successes highlight the utility of AEX methods for quantitation of empty

capsids of serotype specific AAVs, they also clearly show that the separation conditions for each serotype need to be carefully optimized.

Here we report an alternative chromatographic method, not based on separation of empty and full capsids, but based on monitoring the size exclusion eluate using dual-wavelength detection to determine the percent full capsids. The method development and evaluation were performed using a representative AAV5 sample purified by a combination of an AVB Sepharose affinity column and a strong anion exchange column to minimize the presence of empty capsids. As a result, this AAV5 sample contains full capsids in addition to small amounts of empty and partial capsids which co-eluted from the strong anion exchange process column. Spiked samples containing various levels of empty capsids were prepared and evaluated using the newly developed method. The results were subsequently compared to the results obtained from AUC-SV and Cryo-EM studies performed on the same samples.

## Materials and Methods

### Preparation of empty capsids, full capsids, and spiked samples

The empty capsids were purified using a strong anion exchange HQ column. The full capsids were isolated by AVB Sepharose affinity column and HQ anion exchange column, and further purified by cesium chloride density gradient centrifugation to remove any remaining empty and partial capsids and achieve a high purity.

Approximately 20 mL of purified AAV5 virus ( $\sim 5 \times 10^{13}$ – $1 \times 10^{14}$  total vector genomes, transgene size 4.36 kb) was diluted to 30 mL with 20 mM  $\text{NaH}_2\text{PO}_4$ , 400 mM NaCl, 4 mM  $\text{MgCl}_2$ , pH 7.5, to which about 17.8 g of cesium chloride ( $\text{CsCl}_2$ ) was added to bring the final density to 1.35 g/mL. The solution was centrifuged in a Beckman centrifuge equipped with a 70ti rotor at 50,000 rpm overnight at 15°C. Two bands were visible with a dual high intensity fiber light lamp. The upper band and lower band were collected via syringes as the empty and full capsids, respectively. The samples were dialyzed against 1X PBS using 10K MWCO slide-a-lyzers (Thermo Scientific, MA) and then against a buffer consisting of sodium acetate, sodium citrate, sodium chloride, potassium chloride, calcium chloride, magnesium chloride with an osmolality of 200-400 mOsm/kg and a pH of 7.0.

The empty and full capsids were characterized by AUC and droplet digital PCR (ddPCR) and qPCR (Bio-Rad, Hercules, CA) to determine the capsid distribution and vector genome concentration. The concentration of the empty capsid preparation was determined by AAV titration ELISA (Progen, Biotechnik) or  $A_{280}$ . The results are summarized in Table 1.

A series of HPLC standards and spiked samples containing various amounts of full capsid were prepared by mixing the empty and full capsids at defined ratios based on their capsid concentrations (cp/mL). These materials were used to develop the SEC-DW method for empty and full capsids. In addition, for comparison purposes, the samples were evaluated using orthogonal methods such as UV measurements, AUC characterization, and Cryo-EM analyses.

### Extinction coefficients and UV measurements

The extinction coefficient of empty capsids at 280 nm ( $\epsilon_{280, \text{capsid}}$ ) was calculated based on the absorptivity of the aromatic amino acids present in the primary sequences of VP1, VP2 and VP3, using a ratio of VP1:VP2:VP3 of 5:5:50 per capsid. The extinction coefficient of empty capsids at 260 nm ( $\epsilon_{260, \text{capsid}}$ ) was obtained by converting the  $\epsilon_{280, \text{capsid}}$  using a previously published conversion factor of 0.59<sup>16</sup>. The molecular weight (MW) of empty capsids was calculated based on the sequence information and the aforementioned protein ratio. The extinction coefficient of the transgene at 260 nm ( $\epsilon_{260, \text{gene}}$ ) and its MW were calculated based on the gene sequence, and the extinction coefficient at 280 nm ( $\epsilon_{280, \text{gene}}$ ) was then derived with a conversion factor of 0.555<sup>16</sup>. The extinction coefficients at 260 nm and 280 nm of full capsids were the sum of the extinction coefficients of capsid and transgene at each wavelength (e.g.,  $\epsilon_{260, \text{full capsid}} = \epsilon_{260, \text{capsid}} + \epsilon_{260, \text{gene}}$ ). The extinction coefficients of empty and full capsids are summarized in Table 2. The predicted  $A_{260}/A_{280}$  ratio of the different samples used in the study was calculated based on the relative amounts of empty and full capsids present in the samples.

UV absorbance of empty, full and spiked samples was measured using a nanodrop spectrometer (Thermo Fisher, MA).  $A_{260}/A_{280}$  data was plotted against the expected percent full capsids and compared with the predicted  $A_{260}/A_{280}$  data (see Figure S1).

## SEC-DW

AAV capsids (generally 25  $\mu\text{L}$  or 50  $\mu\text{L}$  per injection) were loaded onto a size exclusion column (Sepax SRT SEC-500, 5  $\mu\text{m}$ , 500 $\text{\AA}$ , 7.8 $\times$ 300 mm, Delaware) equipped with a guard column (SRT SEC-500, 5  $\mu\text{m}$ , 500 $\text{\AA}$ , 7.8 $\times$ 50 mm) equilibrated at 25 $^{\circ}\text{C}$  with Dulbecco's phosphate buffered saline without  $\text{CaCl}_2$  and  $\text{MgCl}_2$  (DPBS). In addition to the SEC-500 column, two additional columns (Sepax SRT SEC-300, 5  $\mu\text{m}$ , 300 $\text{\AA}$ , 7.8 $\times$ 300 mm equipped with a guard column SRT SEC-300, 5  $\mu\text{m}$ , 300 $\text{\AA}$ , 7.8 $\times$ 50 mm and Sepax SRT SEC-1000, 5  $\mu\text{m}$ , 1000 $\text{\AA}$ , 7.8 $\times$ 300 mm) equipped with a guard column SRT SEC-1000, 5  $\mu\text{m}$ , 1000 $\text{\AA}$ , 7.8 $\times$ 50 mm) were evaluated for comparison. All columns were run under the same conditions.

The temperature of the autosampler was set at 5 $^{\circ}\text{C}$ . The capsids were eluted with DPBS, pH 7.0 at a flow rate of 0.75 mL/min using an Agilent 1200 series HPLC (Agilent, CA). The eluate was monitored at 260 nm, 280 nm and 230 nm, and data was acquired with the Agilent OpenLab software.

The peak areas of monomeric AAV at 230 nm, 260 nm and 280 nm were used for calculating the peak area (PA) ratios (e.g., PA<sub>260</sub>/PA<sub>230</sub> and PA<sub>260</sub>/PA<sub>280</sub>). The correlation of the peak area ratios with the percent full capsids was established using the HPLC standards and the spiked samples containing various amounts of full capsids.

## AUC-SV

Empty capsids, spiked samples, and full capsids were buffer exchanged into 1X PBS, pH 7.2 (Invitrogen) using 10K MWCO Slide-a-Lyzers or Amicon 10K MWCO centrifugal filters (Millipore Sigma, MO). The absorbance at 260 nm ( $A_{260}$ ) of these samples was measured using a nanodrop spectrometer (Thermo Scientific, MA), to ensure the samples were sufficiently concentrated for the sedimentation experiments ( $0.2 \leq A_{260} \leq 0.6$ ).

**Sedimentation velocity experiment:** The AUC sample (~400  $\mu\text{L}$ ) was loaded into the sample sector of a two sector 1.2 cm Charcoal-filled Epon centerpiece (Beckman Coulter) and PBS (~410  $\mu\text{L}$ ) was loaded into the reference sector. The cells were inserted in a four-hole rotor and equilibrated at full vacuum and 20 $^{\circ}\text{C}$  for at least one hour in the centrifuge

(Optima XL-I, Beckman Coulter). The vectors were sedimented at 20,000 rpm and the absorbance of the vectors was scanned at 260 nm in a continuous mode.

**Data analysis:** The absorbance data was loaded into SEDFIT and fitted with a continuous  $c(s)$  distribution model. The meniscus was floated, and the friction ratio was fixed at 1.0 while fitting the data to the Lamm equation, with time-invariant (TI) and radius-invariant (RI) noise correction. The second-derivative regularization was applied to the fitting with a confidence level of 0.68. A range of 1–200 for sedimentation coefficients was used with a resolution of 200. The published density and viscosity values of PBS were used. The relative abundance of each species in unit of detection was converted to relative abundance in molar concentration by correcting the absorbance according to Beer's Law. The content of each species was reported as a percent of the total. The details on data analysis have been described in the reference<sup>18</sup>.

### Cryo-EM

**Grid preparation:** C-flat holey carbon grids were cleaned with 20 mA for 30 seconds in a Pelco EasiGlow plasma cleaner. Vitriified specimens were prepared by loading a grid into a manual plunger (EMS-002 Rapid Immersion Freezer), adding 4  $\mu$ L of virus to the grid, immediately one-side blotting the grid for 2 seconds, and freezing the sample in liquid ethane.

**Imaging:** Electron microscopy was performed by the Core Facility of UMass Medical School using a Titan Krios electron microscope operated with an accelerating voltage at 300 kV and equipped with a K3 direct electron detector. Data was collected using SerialEM at 105,000 $\times$  nominal magnification (pixel size of 0.83 $\text{\AA}$ ) at 2.5  $\mu$ m defocus and a dose of  $\sim 48.0 e^-/\text{\AA}^2$ .

**Data analysis:** An in-house data analysis software program developed at the Cryo-EM Core Facility of UMass Medical School was used to recognize and count the empty and full capsids. For quantitation of the percent full capsids, many images were processed and a total of approximately 2,200–8,700 vectors were analyzed and counted as empty and full capsids for each spiked sample. The content of full capsids from all the images analyzed for each sample was reported as a percent of the total capsids.



## Results

### Initial column screening

The selection of a suitable column to perform SEC analysis of AAV capsids is primarily dictated by the molecular properties of the capsids and the column chemistry. The molecular weight of AAV capsids is 3.5–6.0 megadaltons and the capsids have a diameter of 20–25 nm. Therefore, SEC resins with a pore size from 300 to 1,000 Å (30 to 100 nm) would be suitable for separating monomeric AAVs from aggregated species as well as from low molecular weight species and small molecules that are expected to be present in a sample. To avoid any possible sieving effect, an analytical column with a large inner diameter packed with a stationary phase consisting of a relatively large particle size would be preferred. Indeed, several vendors including Waters, Sepax and Wyatt manufacture columns that may be suitable for this purpose. Sepax SRT SEC columns are packed with spherical high purity silica coated with nanometer thick hydrophilic and neutral films and these materials have shown promise for separation of virus and virus-like particles. Three columns with preferred column dimensions (300×7.8 mm) and particle size (5 µm), but different pore sizes (300, 500 and 1,000 Å) were evaluated for their performance to analyze AAV5 containing samples using phosphate buffered saline (PBS) as the mobile phase. The chromatograms of AAV5 samples are shown in Figure 1. The monomeric vectors eluted from the column with the retention time increasing in the order of increased pore size, manifesting the diffusion characteristics of the solute inside and outside of different micropores (Figure 1A). The monomer peak observed in the elution profile obtained for the SEC-300 column is sharp but slightly skewed, and the trace amount of aggregates, which is expected to elute prior to the monomer peak, was not observed. The elution profile obtained for the SEC-1000 column (Figure 1A) shows the monomer eluting too close to the peak representing low molecular weight species (buffer peaks). The SRT SEC-500 column with a 500 Å pore size was therefore selected for further development as the retention time, peak shape and resolution are satisfactory. As shown in Figure 1B, the peak area representing the monomer is higher when the signal is monitored at 260 nm compared to 280 nm resulting in a peak area ratio (PA<sub>260</sub>/PA<sub>280</sub>) of approximately 1.25 which is indicative of a sample containing mostly full capsids. The

minor peaks eluting at approximately 5.8 mins and 8.6 mins are AAV aggregates (0.5% for HMWS 1 and 1.7% for HMWS 2), indicating that the method is capable of detecting low level aggregates, which can create undesired consequences on transduction efficiency, biodistribution, and immunogenicity. When different volumes (10–75  $\mu\text{L}$  of  $5 \times 10^{12}$  cp/mL) of the DS sample were injected, excellent linearity was observed ( $R^2 = 0.997$ ) for the peak areas at 260 nm and 280 nm in relation to the number of capsids injected (Figure 1C), and the PA260/PA280 ratio remained unchanged over the range tested, suggesting that the titer of the sample could be determined.

### SEC with dual-wavelength detection for the AAV spiked samples

The various capsid standards and samples were initially monitored at 260 nm and 280 nm as shown in Figure 1A, where encapsidated nucleic acids and capsid proteins have their absorbance maxima, respectively<sup>24</sup>. The SEC chromatograms of the HPLC standard samples in Figure 2A and B show that the monomers are well-resolved from the small aggregate peaks. The PA260/PA280 ratios obtained for the standard samples are plotted against the expected value for the percent full capsids calculated based on the ratio of the empty and full capsid stock solutions combined to prepare the samples (Figure 2D). As shown in Figure 2D, the PA260/PA280 ratio approaches an asymptote when the full capsids account for more than 70% of total capsids. As a result, the method has limited capability to determine the percent full capsids with appropriate accuracy and precision when the full capsid content is greater than 70%. A similar limitation was previously observed when using UV spectroscopy to monitor the  $A_{260}/A_{280}$  ratios<sup>16</sup>. The  $A_{260}/A_{280}$  ratios of the spiked samples are shown in supporting information Figure S1. As gene therapy candidates often have more than 70% full capsids in the drug substance and drug product, owing to the continuous improvements of the upstream and downstream processes, a method capable of accurately monitoring percent full capsids greater than 90% is required.

To extend the range of the method the use of other wavelengths was evaluated. It was hypothesized that the absorbance of capsid proteins would be much more intense and become dominant at the 230 nm wavelength, while the contributory absorbance of transgenes would be limited (e.g., absorbance of nucleic acids has a trough at 230 nm, and the  $A_{260}/A_{230}$  ratio for pure nucleic acids is typically in the range of 1.8–2.2<sup>25</sup>). Figure 2C

shows the SEC traces of the standards at 230 nm. As hypothesized, the peak area monitored at 260 nm and 230 nm is proportional to the column loading and the PA260/PA230 ratio remains constant over the range tested, confirming that the intrinsic PA260/PA230 ratio is independent of the capsid concentration (see supporting information Figure S2). By using this new dual wavelength for detection and calculation of the peak area ratios, a linear relationship between PA260/PA230 and percent full capsids was established ( $y = 0.0057x + 0.1137$ ). The goodness of fit was excellent, judged by the  $R^2$  of 0.999 (Figure 2D). The ability to use a linear curve fit when using the PA260/PA230 ratio versus the percent full capsid is critical as such a change allows the extension of the assay range beyond 70% full capsids. The full capsid sample used in this study contains 91% full and 9% partial capsids, and therefore it was not possible to evaluate the capability of the method above this level. The assay range may potentially be extended to near 100% full capsids, given the linear relationship observed. Due to the nature of SEC chromatography this analysis can be performed using only a small volume (e.g., 10–50  $\mu$ L) at capsid concentrations of  $\sim 5 \times 10^{12}$  cp/mL. In addition, the method also normalizes the pH and ionic strength of the sample to match the pH and ionic strength of the mobile phase, and therefore minimizes their impact on the absorbance of transgenes<sup>26</sup>.

### **Specificity, reproducibility, and robustness of SEC-DW**

The SEC-DW method separates the AAV capsids from the excipients and/or buffer components (Figure 2), thus the components in the formulation buffer are not expected to have any impact on the PA260/PA230 ratio. The Bio-Rad's gel filtration standard containing thyroglobulin,  $\gamma$ -globulin, ovalbumin, myoglobin, and vitamin B<sub>12</sub> was used to estimate what size of proteins may interfere with the analysis. Bovine thyroglobulin eluted at a retention time window of 8–13 mins, indicating that only proteins of this size (MW 670,000 Da) and higher would potentially interfere with the quantitation of empty and full capsids (data not shown). This type of protein impurities is not expected to be present at a significant level in the samples post affinity and/or strong anion exchange column purification. The injections of the mobile phase blank after 14 injections of AAV samples showed no detectable peaks by both wavelengths near the retention time of monomeric AAV5, indicating no carryover from the previous injections. The SEC-DW method was used

to determine the percent full capsids in the drug substance (DS) and working reference standard (WRS) generated as part of an AAV5 development program. Samples were compared against a standard curve generated using HPLC standards containing different ratios of the empty and full capsids (Figure 2D). The analysis was then performed over multiple assay occasions (different mobile phase lots) on different days. The PA260/PA230 values were 0.55 (n = 8), 0.57 (n = 4), and 0.11 (n = 6) for the DS, WRS and empty capsid samples. The results indicated that the DS and the WRS samples contained approximately 76% and 83% full capsids, respectively (Figure 2E), similar to the results obtained by AUC-SV. The percent full capsids for the empty capsid sample was 0% (the actual value calculated based on the linear equation established was -1.1%). The %RSD values of the PA260/PA230 ratios and % full capsids for the DS sample (n = 8) and the WRS sample (n = 4) are less than 1%, demonstrating that the results are highly reproducible over different assays, different mobile phase lots and different days.

The spiked samples prepared separately using the empty and full capsids stocks led to a similar linear equation ( $y = 0.0057x + 0.1195$ ) between the PA260/PA230 ratios and the percent full capsids and a  $R^2$  value of 0.999. The same slope and similar intercept again manifest the consistency of the SEC-DW method. Both constants  $a$  and  $b$  for the linear equation ( $y = ax + b$ ) are indeed related to the intrinsic optical properties of the vector.

To gain understanding of the effect of changes in method parameters, the pH and flow rate of the mobile phase were deliberately varied during the development (three pH values at 6.6, 7.0, and 7.5, and three flow rates at 0.70, 0.75, and 0.80 mL/min). The PA260/PA230 values of the same DS sample were 0.55 under all three pH conditions and were 0.54 at the three flow rates. The percent full capsids were in the range of 74.8–76.4%, again using the linear equation established. These results demonstrate that the SEC-DW method is robust within the variations tested.

### **Percent full capsids by AUC-SV**

To further examine the suitability of the SEC-DW method for empty and full capsids, the spiked samples were dialyzed and then analyzed by AUC-SV using the method previously developed by O’Riordan and coworkers<sup>18</sup>. The sedimentation of vectors was monitored at

260 nm along the centrifugal field in a continuous mode, and the acquired data were fitted to the Lamm equation using the computer program SEDFIT<sup>27</sup>. The representative sedimentation coefficient distribution  $c(s)$  plots for four samples (empty, two spiked samples and full capsids) are shown in Figure 3.

Different species including empty, partial and full capsids, as well as high molecular weight species were detected and can be identified based on their sedimentation coefficients (approximately 64–66S for empty capsids, 80–90S for partial capsids, and 101–107S for full capsids with a transgene of ~4,360 nucleotides). Integration of each peak resulted in the relative percentage of each species in unit of detection, which was converted to the molar concentration of each species according to Beer's Law due to the considerable differences in the extinction coefficients at 260 nm of the individual species<sup>18</sup>.

Figure 3A shows the sedimentation coefficient distribution plot for the subpopulations of the empty capsid sample (98% empty capsids (65S) and 2% partial capsids (81S)). The results for the full capsid sample purified via cesium chloride density gradient centrifugation are shown in Figure 3D and indicate that the sample contains 91% full capsids (104S) and 9% partial capsids (88S). The partial capsids with a sedimentation coefficient of 88S represent capsids harboring fragmented genomes of approximately 2,700 nucleotides<sup>28</sup>. On a separate AUC-SV analysis, the subpopulations of the empty capsid sample are 99% empty (65S) and 1% partial capsids (83S), the subpopulations of the full capsid sample are 8% partial (86S) and 92% full capsids (101S), demonstrating the consistency between the AUC-SV runs. Figure 3B and Figure 3C represent samples which were prepared by mixing the full and empty capsid containing samples. The % full capsid for these samples was calculated as 55% and 82% full capsids, respectively, based on the assigned values for the full and empty capsid samples and the combined volumes. The full capsid contents are 52% and 88% by AUC-SV for these two samples. The results from the SEC-DW method (approximately 58% and 81% for these two samples) are in very good agreement with the AUC-SV results. A small fraction of partial capsids is present for all samples, particularly in the full capsid sample despite the stringent purification efforts. The presence of partial capsids manifests the challenge of producing drug substance that mainly consists of full capsids. The partial capsids cannot be discerned by AEX, SEC and

TEM methods, but are well distinguished by AUC-SV, showcasing the high hydrodynamic resolving power of AUC-SV. In addition, the samples recovered from AUC-SV experiments were re-analyzed by SEC-DW directly with a 25  $\mu$ L injection. Similar chromatographic profiles and percent full capsid results were obtained (data not shown), confirming that all the capsids remained intact post AUC-SV experiments.

### **Percent full capsids by Cryo-EM**

Cryo-electron microscopy is an electron microscopy technique that can measure empty and full capsids in their frozen hydrated state<sup>29</sup>. Vitrified capsids were prepared by freezing them in liquid ethane, and electron microscopy images were collected using a Titan Krios. One of the Cryo-EM images taken for the spiked sample containing approximately 55% full capsids is shown in Figure 4A, in which the representative full capsid (displaying significant internal density) and empty capsid (absence of internal density) are circled and both the empty and full capsids are similar in size (approximately 24 nm).

Figure 4B is selected from the images for the full capsid sample, and almost no empty capsids can be identified. For each spiked sample, at least 2,200 particles from multiple images were counted using in-house data analysis software (Cryo-EM core facility of UMASS Medical School). The results from all images analyzed were combined to calculate the percentage of full capsids and ensure statistical significance. Partial capsids were treated as full capsids by Cryo-EM analyses in this study, although they can be identified by Cryo-EM via 3D classification<sup>29</sup>. The percentages of full capsids for the empty, spiked samples and full capsid sample are 3, 24, 37, 54, 81, 88 and 97%. The number of images analyzed, the total number of full capsids, the total number of empty capsids, the number of particles counted with low confidence (artifact, background signal. etc.), and the percent full capsids in the samples by Cryo-EM are summarized in Table 3. The SEC-DW results are similar to the percent full capsids measured by Cryo-EM, and thus provides a viable option for GMP testing.

### **Comparison of percent full capsids determined by SEC-DW, AUC-SV and Cryo-EM**

To scientifically validate the SEC-DW method, we compared the percent full capsids determined by SEC-DW with the results from two state-of-the-art high-resolution

methods: AUC-SV and Cryo-EM which can accurately measure the percent full capsids. These three methods all characterize the AAV samples in their native state: in solution passing through the column for SEC-DW, free in solution in a centrifugal field for AUC-SV, and in frozen hydrated state after flash-freezing for Cryo-EM. The percent full capsids of the spiked samples determined by SEC-DW, AUC-SV and Cryo-EM are illustrated in Figure 5. The results from all three methods demonstrate excellent linearity between the observed and expected percent full capsids (Figure 5A), judged by the  $R^2$  values from the linear regressions (0.997, 0.993, and 0.993 for SEC-DW, AUC-SV and Cryo-EM). The slopes of the linear regressions are 0.989, 1.062, and 1.038 for SEC-DW, AUC-SV and Cryo-EM, indicating that the SEC-DW method does not have any significant bias when compared to the AUC-SV and Cryo-EM methods. Partial capsids are treated as full capsids by Cryo-EM in this study, thus, the reported full capsids for each sample are slightly higher than those values from AUC-SV (Figure 5B). Overall, the percent full capsids by SEC-DW based on PA260/PA230 agree very well with the results from AUC-SV and Cryo-EM (Figure 5B) across the whole range tested (0–91% full capsids, or 0–98% empty capsids), demonstrating the SEC-DW method is accurate and reliable.

## Discussion

The SEC-DW method developed in this study for determining the relative amounts of empty and full capsid uses common HPLC equipment that is readily available in development and QC labs, directly quantifies the percent full capsids in a sample, requires small sample amounts (10–75  $\mu\text{L}$  of  $5 \times 10^{12}$  cp/mL sample per injection), provides the highest throughput among the three methods, and can be qualified/validated for cGMP use. The SEC-DW method does not need additional sample preparations such as denaturation and labeling, and the impact of matrices are effectively eliminated during the size exclusion elution. The matrix effect becomes significant particularly when the detection wavelength is shifted from 280 nm to 230 nm for capsid proteins. The presence of partial capsids is inevitable from the current manufacturing processes. The gene sequences packaged in the partial capsids do contribute to the absorbance at 260 nm and 230 nm, and therefore introduce some variations to the reportable results. Some of these variations are built in the linear equation initially established and therefore the impact of

partial capsids on the quantitation of the percent full capsids is limited. Nevertheless, SEC-DW, similar to other chromatographic methods, cannot distinguish partial capsids, and they may have to be characterized by other complementary methods for the encapsidated DNA and the potential expression of these genes, if required. Another concern is the impact of the light scattering on the absorbance of vectors. The light scattered by a spherical solute is inversely proportional to  $\lambda^4$ , according to Rayleigh approximation. The light scattering can be corrected for absorbance at 230 nm and 260 nm using the wavelength dependent extrapolation. The absorbance spectra of empty and full capsids at 220–400 nm were extracted from the data acquired by the photodiode array (PDA) detector and no significant light scattering was observed based on the minimal to neglectable absorbance at 320–360 nm (see Supporting information Figure S3 and Figure S4). We established this SEC-DW method using AAV5 DS samples (see Supporting information Figure S4 for results of an AAV5 drug candidate 2), but it should be applicable for testing in-process samples as long as there is no interference from any other macromolecules that may elute as monomeric AAVs. If necessary, the in-process samples can be readily concentrated with a centrifugal concentrator to ensure a proper capsid concentration. This SEC-DW method may potentially be applied to other AAV serotypes once the linear relationship of PA260/PA230 vs. percent full capsids is established. The protein detection wavelength of 230 nm can be adjusted if necessary, in the search of such a linear relationship. AUC-SV appears to be most suitable for characterization of all subpopulations of capsids including partial capsids owing to its high hydrodynamic resolution. Indeed, O’Riordan et al. revealed that the size of genomes (2.1– 4.3 kb) packaged in the vectors correlated well with sedimentation coefficients of the vectors<sup>18</sup>. This capability renders AUC-SV a powerful investigational and characterization tool for understanding the packaging difference during the upstream process development. However, the instrument and data analysis requirements, the low throughput, and the sample volume requirements make the implementation of this method difficult for routine testing especially when large number of samples need to be analyzed. Cryo-EM quantifies percent full capsids with high accuracy when a sufficient number of viral particles are evaluated<sup>30</sup>. The damage of capsids due to hydration or false staining that could occur in TEM do not happen in Cryo-EM<sup>31</sup>. Cryo-EM requires less than 10  $\mu\text{L}$  of  $5 \times 10^{12}$  cp/mL



sample and data analysis has been mostly automated. Similar to AUC-SV, Cryo-EM is a low throughput method requiring specially trained analysts creating a significant impediment to its implementation in a QC environment and/or a development lab. Considering the sample and instrument requirements, the SEC-DW method can prove useful for determining empty and full capsid contents on a readily accessible instrument platform in a high throughput manner.

### **Conclusion**

Size exclusion chromatography with dual wavelength detection at 260 nm and 230 nm is a direct, reproducible, and accurate approach to determine the relative proportion of empty and full capsids in rAAV samples. The use of a detection wavelength of 230 nm for capsid proteins, instead of 280 nm, to normalize the transgene signal at 260 nm results in a linear relationship between PA260/PA230 and the percent full capsids. This non-conventional dual wavelength detection significantly increases the range of the assay and enables accurate quantitation for rAAV samples which typically contain low levels of empty capsids. Our results have shown that the range can be increased up to 91% full capsids (or full capsids equivalent), and probably higher if an appropriate composition could be tested. The accuracy of this SEC-DW method was confirmed based on a comparison to the results obtained using the orthogonal high-resolution methods AUC-SV and Cryo-EM. The method would be applicable to multiple serotypes, for which a linear relationship between PA260/PA230 and percent full capsids can be established. Since the method relies on standard HPLC analysis conditions and equipment, the method can be readily implemented as a QC release method after qualification, or as a rapid monitoring tool to support process development and product understanding.

### **Supplemental information**

Supplemental information can be found with this article online.

### **Acknowledgement**

We thank our colleagues Jarrod Dean at analytical development, Jason Morais and Simon Godwin at the gene therapy skill center, and Xiaoying Jin at characterization group for their help and discussions. We thank Prof. Chen Xu and Dr. KyoungHwan Lee of Cryo-EM Core

Facility at University of Massachusetts Medical School for Cryo-EM data collection and analysis.

### **Author disclosure**

All authors are employees of Sanofi and may hold shares and/or stock options in the company.

### **Funding information**

Funding of this work was provided entirely by Sanofi.

## References

1. Naso, M. F.; Tomkowicz, B.; Perry, W. L., 3rd; Strohl, W. R., Adeno-Associated Virus (AAV) as a Vector for Gene Therapy. *BioDrugs* **2017**, *31* (4), 317-334.
2. Daya, S.; Berns, K. I., Gene therapy using adeno-associated virus vectors. *Clin Microbiol Rev* **2008**, *21* (4), 583-93.
3. Li, C.; Samulski, R. J., Engineering adeno-associated virus vectors for gene therapy. *Nat Rev Genet* **2020**, *21* (4), 255-272.
4. Russell, S.; Bennett, J.; Wellman, J. A.; Chung, D. C.; Yu, Z. F.; Tillman, A.; Wittes, J.; Pappas, J.; Elci, O.; McCague, S.; Cross, D.; Marshall, K. A.; Walshire, J.; Kehoe, T. L.; Reichert, H.; Davis, M.; Raffini, L.; George, L. A.; Hudson, F. P.; Dingfield, L.; Zhu, X.; Haller, J. A.; Sohn, E. H.; Mahajan, V. B.; Pfeifer, W.; Weckmann, M.; Johnson, C.; Gewaily, D.; Drack, A.; Stone, E.; Wachtel, K.; Simonelli, F.; Leroy, B. P.; Wright, J. F.; High, K. A.; Maguire, A. M., Efficacy and safety of voretigene neparvovec (AAV2-hRPE65v2) in patients with RPE65-mediated inherited retinal dystrophy: a randomised, controlled, open-label, phase 3 trial. *Lancet* **2017**, *390* (10097), 849-860.
5. Wang, D.; Tai, P. W. L.; Gao, G., Adeno-associated virus vector as a platform for gene therapy delivery. *Nature reviews. Drug discovery* **2019**, *18* (5), 358-378.
6. Wright, J. F., Product-Related Impurities in Clinical-Grade Recombinant AAV Vectors: Characterization and Risk Assessment. *Biomedicines* **2014**, *2* (1), 80-97.
7. Qu, G.; Bahr-Davidson, J.; Prado, J.; Tai, A.; Cataniag, F.; McDonnell, J.; Zhou, J.; Hauck, B.; Luna, J.; Sommer, J. M.; Smith, P.; Zhou, S.; Colosi, P.; High, K. A.; Pierce, G. F.; Wright, J. F., Separation of adeno-associated virus type 2 empty particles from genome containing vectors by anion-exchange column chromatography. *J Virol Methods* **2007**, *140* (1-2), 183-92.
8. Wright, J. F., Manufacturing and characterizing AAV-based vectors for use in clinical studies. *Gene Ther* **2008**, *15* (11), 840-8.

9. Gao, K.; Li, M.; Zhong, L.; Su, Q.; Li, J.; Li, S.; He, R.; Zhang, Y.; Hendricks, G.; Wang, J.; Gao, G., Empty Virions In AAV8 Vector Preparations Reduce Transduction Efficiency And May Cause Total Viral Particle Dose-Limiting Side-Effects. *Mol Ther Methods Clin Dev* **2014**, *1* (9), 20139.
10. Mingozi, F.; Anguela, X. M.; Pavani, G.; Chen, Y.; Davidson, R. J.; Hui, D. J.; Yazicioglu, M.; Elkouby, L.; Hinderer, C. J.; Faella, A.; Howard, C.; Tai, A.; Podsakoff, G. M.; Zhou, S.; Basner-Tschakarjan, E.; Wright, J. F.; High, K. A., Overcoming preexisting humoral immunity to AAV using capsid decoys. *Science translational medicine* **2013**, *5* (194), 194ra92.
11. Wright, J. F., AAV empty capsids: for better or for worse? *Mol Ther* **2014**, *22* (1), 1-2.
12. Schnodt, M.; Buning, H., Improving the Quality of Adeno-Associated Viral Vector Preparations: The Challenge of Product-Related Impurities. *Hum Gene Ther Methods* **2017**, *28* (3), 101-108.
13. Flotte, T. R., Empty Adeno-Associated Virus Capsids: Contaminant or Natural Decoy? *Hum Gene Ther* **2017**, *28* (2), 147-148.
14. EMA, Guideline on the quality, non-clinical and clinical aspects of gene therapy medicinal products. 2018; p EMA/CAT/80183/2014.
15. FDA, Guidance for Industry Chemistry, Manufacturing, and Control (CMC) Information for Human Gene Therapy Investigational New Drug Applications (INDs). 2020.
16. Sommer, J. M.; Smith, P. H.; Parthasarathy, S.; Isaacs, J.; Vijay, S.; Kieran, J.; Powell, S. K.; McClelland, A.; Wright, J. F., Quantification of adeno-associated virus particles and empty capsids by optical density measurement. *Mol Ther* **2003**, *7* (1), 122-8.
17. Takahashi, E.; Cohen, S. L.; Tsai, P. K.; Sweeney, J. A., Quantitation of adenovirus type 5 empty capsids. *Analytical biochemistry* **2006**, *349* (2), 208-17.
18. Burnham, B.; Nass, S.; Kong, E.; Mattingly, M.; Woodcock, D.; Song, A.; Wadsworth, S.; Cheng, S. H.; Scaria, A.; O'Riordan, C. R., Analytical Ultracentrifugation as an Approach to Characterize Recombinant Adeno-Associated Viral Vectors. *Hum Gene Ther Methods* **2015**, *26* (6), 228-42.

19. Pierson, E. E.; Keifer, D. Z.; Asokan, A.; Jarrold, M. F., Resolving Adeno-Associated Viral Particle Diversity With Charge Detection Mass Spectrometry. *Anal Chem* **2016**, *88* (13), 6718-25.
20. Li, T.; Gao, T.; Chen, H.; Pekker, P.; Menyhart, A.; Guttman, A., Rapid determination of full and empty adeno-associated virus capsid ratio by capillary isoelectric focusing. *Curr Mol Med* **2020**.
21. Lock, M.; Alvira, M. R.; Wilson, J. M., Analysis of particle content of recombinant adeno-associated virus serotype 8 vectors by ion-exchange chromatography. *Hum Gene Ther Methods* **2012**, *23* (1), 56-64.
22. Fu, X.; Chen, W. C.; Argento, C.; Clarner, P.; Bhatt, V.; Dickerson, R.; Bou-Assaf, G.; Bakhshayeshi, M.; Lu, X.; Bergelson, S.; Pieracci, J., Analytical Strategies for Quantification of Adeno-Associated Virus Empty Capsids to Support Process Development. *Hum Gene Ther Methods* **2019**, *30* (4), 144-152.
23. Wang, C.; Mulagapati, S. H. R.; Chen, Z.; Du, J.; Zhao, X.; Xi, G.; Chen, L.; Linke, T.; Gao, C.; Schmelzer, A. E.; Liu, D., Developing an Anion Exchange Chromatography Assay for Determining Empty and Full Capsid Contents in AAV6.2. *Mol Ther Methods Clin Dev* **2019**, *15*, 257-263.
24. Porterfield, J. Z.; Zlotnick, A., A simple and general method for determining the protein and nucleic acid content of viruses by UV absorbance. *Virology* **2010**, *407* (2), 281-8.
25. Desjardins, P.; Conklin, D., NanoDrop microvolume quantitation of nucleic acids. *J Vis Exp* **2010**, (45).
26. Wilfinger, W. W.; Mackey, K.; Chomczynski, P., Effect of pH and ionic strength on the spectrophotometric assessment of nucleic acid purity. *Biotechniques* **1997**, *22* (3), 474-6, 478-81.
27. Brown, P. H.; Schuck, P., Macromolecular size-and-shape distributions by sedimentation velocity analytical ultracentrifugation. *Biophys J* **2006**, *90* (12), 4651-61.

28. Nass, S. A.; Mattingly, M. A.; Woodcock, D. A.; Burnham, B. L.; Ardinger, J. A.; Osmond, S. E.; Frederick, A. M.; Scaria, A.; Cheng, S. H.; O'Riordan, C. R., Universal Method for the Purification of Recombinant AAV Vectors of Differing Serotypes. *Mol Ther Methods Clin Dev* **2018**, *9*, 33-46.
29. Subramanian, S.; Maurer, A. C.; Bator, C. M.; Makhov, A. M.; Conway, J. F.; Turner, K. B.; Marden, J. H.; Vandenberghe, L. H.; Hafenstein, S. L., Filling Adeno-Associated Virus Capsids: Estimating Success by Cryo-Electron Microscopy. *Hum Gene Ther* **2019**, *30* (12), 1449-1460.
30. Kronenberg, S.; Kleinschmidt, J. A.; Bottcher, B., Electron cryo-microscopy and image reconstruction of adeno-associated virus type 2 empty capsids. *EMBO Rep* **2001**, *2* (11), 997-1002.
31. Adrian, M.; Dubochet, J.; Lepault, J.; McDowell, A. W., Cryo-electron microscopy of viruses. *Nature* **1984**, *308* (5954), 32-6.

Table 1 Capsid concentration, vector genome concentration and subpopulation distribution of empty and full capsids

Samples	Capsids conc. (cp/mL)	Vector genome conc. (vg/mL)	Empty capsids (%)	Partial capsids (%)	Full capsids (%)
Empty capsids	$1.21 \times 10^{13}$	$2.50 \times 10^{11}$	98	2	0
Full capsids	$4.95 \times 10^{12}$	$4.50 \times 10^{12}$	0	9	91

Table 2 Theoretical extinction coefficients of empty capsids and full capsids

$\epsilon_{280}$ , empty capsid ( $M^{-1} \cdot cm^{-1}$ )	$\epsilon_{260}$ , empty capsid ( $M^{-1} \cdot cm^{-1}$ )	$\epsilon_{280}$ , full capsid ( $M^{-1} \cdot cm^{-1}$ )	$\epsilon_{260}$ , full capsid ( $M^{-1} \cdot cm^{-1}$ )
6,768,550.0	3,993,444.5	21,731,437.4	30,953,601.9



Table 3 Percent full capsids determined by Cryo-EM for the spiked samples

Samples	Number of full capsids	Number of empty capsids	Particles with low confidence	Number of images	Total number of full and empty capsids	Full capsids (%)
Empty	85	3287	247	48	3372	2.5
Spiked 1	1322	4210	447	114	5532	23.9
Spiked 2	1482	2563	466	99	4045	36.6
Spiked 3	2487	2120	258	45	4607	54.0
Spiked 4	1805	426	533	104	2231	80.9
Spiked 5	2633	345	220	64	2978	88.4
Full	8447	260	317	95	8707	97.0

## FIGURE LEGENDS

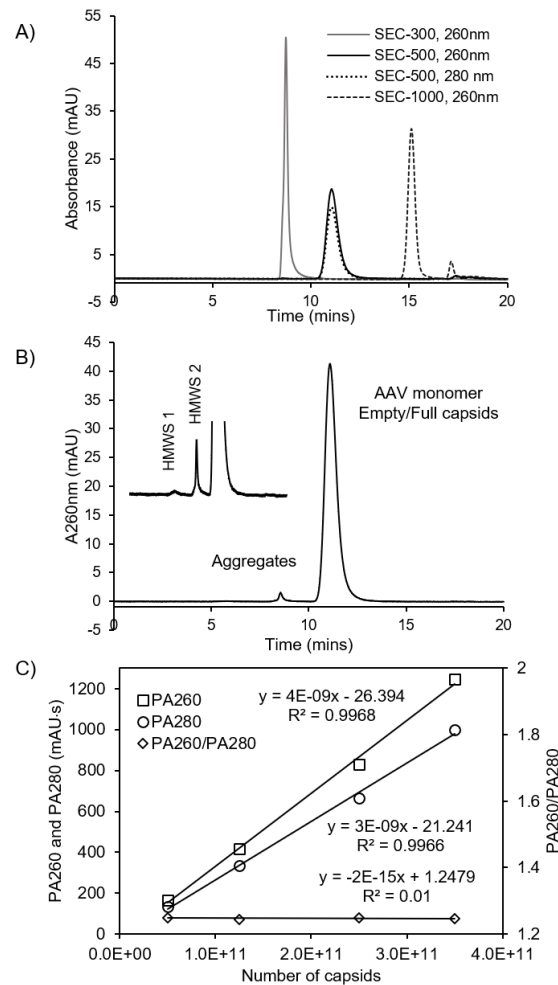


Figure 1 A) SEC chromatograms of an AAV5 DS sample. The DS sample was diluted with Dulbecco's phosphate buffered saline (DPBS) to approximately  $5.0 \times 10^{12}$  cp/mL and 25  $\mu$ L of HPLC sample was applied onto the column. The elution was monitored with a photodiode array (PDA) detector. SEC-300 column (gray trace), SEC-500 column (black trace at 260 nm, dotted black trace at 280 nm), and SEC-1000 column (dashed gray trace). For SEC-300 and SEC-1000, only traces at 260 nm were shown for clarity. B) Chromatogram of a different lot of DS sample showing aggregated AAVs and monomer at 260 nm resolved by the SEC-500 column. The inset shows the high molecular weight species 1 (HMWS 1, 0.5% by peak area) and high molecular weight species 2 (HMWS 2, 1.7%). C) The peak areas detected at 260 nm and 280 nm show a linear relationship with the number of capsids injected. PA260/PA280 remains constant across the range tested ( $5.0 \times 10^{10}$  to  $3.5 \times 10^{11}$  capsids, 10–75  $\mu$ L injection of  $5.0 \times 10^{12}$  cp/mL).

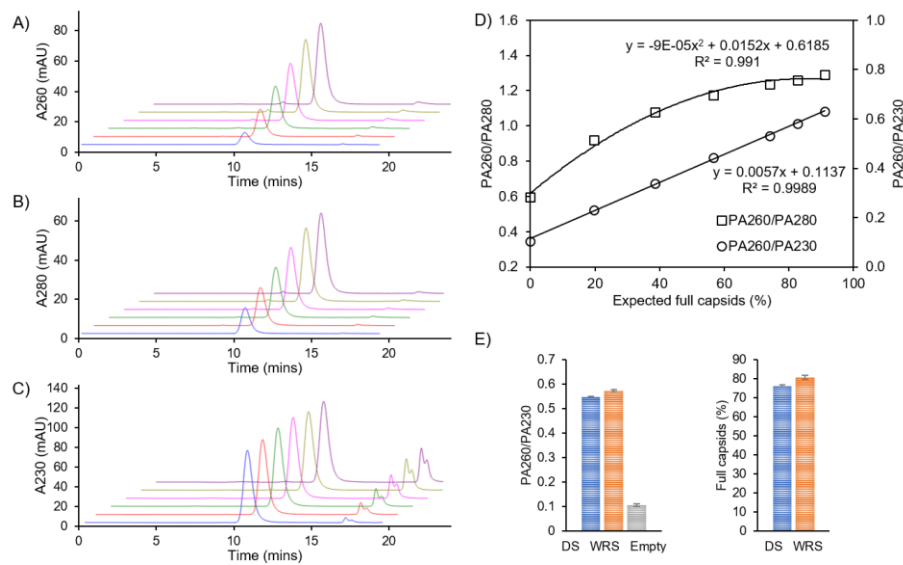


Figure 2 A) Chromatograms of a series of AAV5 HPLC standards containing various percentages of full capsids at 260 nm. From front to back, the empty capsids, spiked samples with increased amount of full capsids from approximately 20% to 80%, and full capsids (91% full and 9% partial). B) Chromatograms of the empty, spiked samples and full capsids at 280 nm. C) Chromatograms of the empty, spiked samples, and full capsids at 230 nm. Chromatograms of one of the standard samples were not shown as the loading led to different absorbance intensities. D) The peak area ratios at 260 nm and 280 nm (PA260/PA280) and the peak area ratios at 260 nm and 230 nm (PA260/PA230) by SEC for the AAV5 samples. The curve fitting function changed from quadratic (for PA260/PA280, y-axis on the left) to linear regression (for PA260/PA230, y-axis on the right), which effectively extended the assay range. E) The PA260/PA230 ratio of the AAV5 drug substance (n = 8), working reference standard (WRS, n = 4), and empty capsids (n = 6) samples obtained from multiple assay occasions performed on different days. The percent full capsids in the DS (n = 8) and WRS (n = 4) samples were calculated based on the linear relationship established between the PA260/PA230 and the percent full capsids ( $y = 0.0057x + 0.1137$ ). The %RSD values are 0.58%, 0.54% and 5.30% for the PA260/PA230 values of the DS, WRS and empty capsids samples. The %RSD values are 0.73% and 0.67% for the percent full capsids of the DS and WRS samples, respectively. These results demonstrate the excellent intermediate precision of the method.

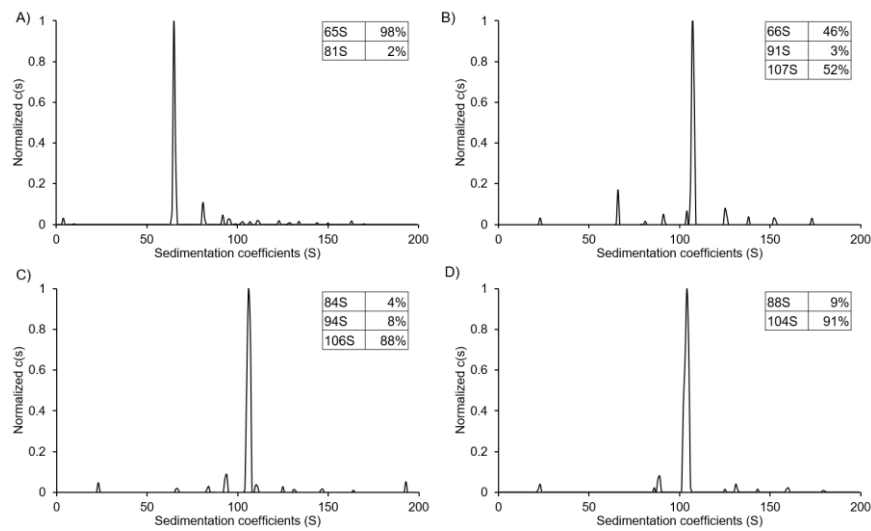


Figure 3 Representative AUC-SV data are shown as sedimentation coefficient distribution plots of empty capsids (A), spiked sample 3 (B), spiked sample 5 (C), and full capsids (D). The sedimentation of AAV particles was monitored at 260 nm. The raw data were fitted with the Lamm equation using the  $c(s)$  model in SEDFIT. The x axis represents the sedimentation coefficient in Svedberg units (S), and the y axis represents the concentration as a function of the sedimentation coefficient. Two abundant and distinct populations of virions were observed: full capsids with a sedimentation coefficient of approximately 101–107S, and empty capsids with a sedimentation coefficient of 64–66S. Partial capsids with a sedimentation coefficient of 81–94S were present in all the samples, at a much lower level compared to the empty and full capsids. In addition, a trace amount of high molecular weight species was evident. These high molecular weight species were not included in the quantitation of the overall empty, partial and full capsids.

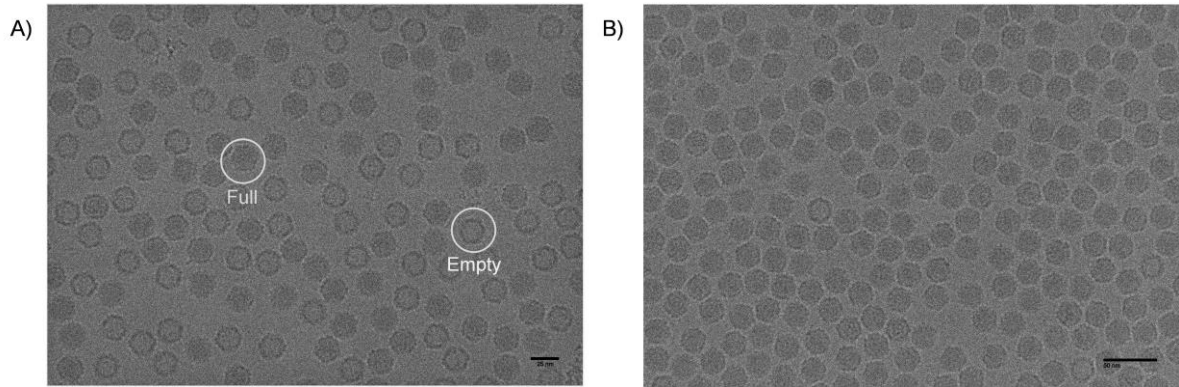


Figure 4 Representative Cryo-EM images of two spiked samples. A) Image of the spiked sample 3 containing 54% full capsids by Cryo-EM; B) Image of the full capsid sample containing 97% full capsids by Cryo-EM. An empty capsid and a full capsid are indicated in Image A. Cross sections of empty capsids can be distinguished by their well-defined border due to their lower internal density. Cross sections of full capsids have a more homogenous appearance due to their significant internal density.

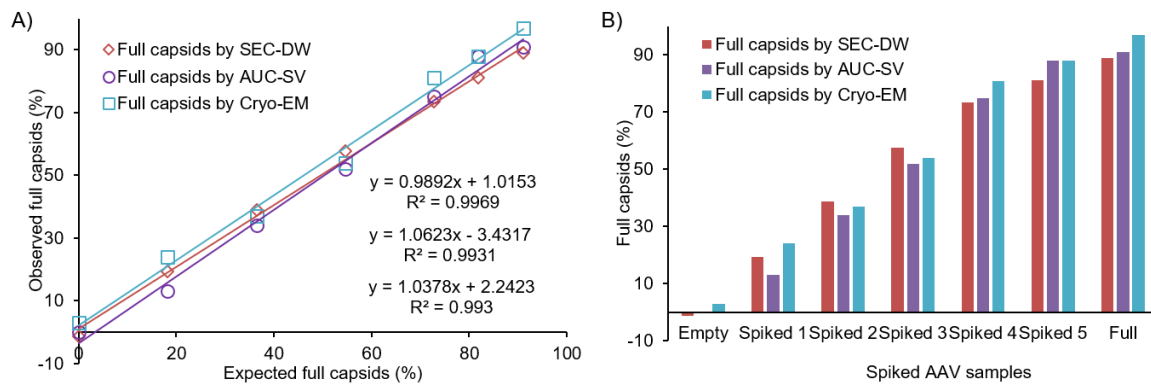


Figure 5 A) The percent full capsids in the spiked samples obtained from SEC-DW, AUC-SV, and Cryo-EM. The results were plotted against the expected percent full capsids and fitted with linear regressions. The  $R^2$  values are 0.997, 0.993 and 0.993 for SEC-DW, AUC-SV, and Cryo-EM, indicating excellent linearity for all three methods. The slope values are 0.9892 for SEC-DW, 1.0623 for AUC-SV, and 1.0378 for Cryo-EM, demonstrating no significant bias for all three methods. B) The results from SEC-DW, AUC-SV, and Cryo-EM are presented as a bar graph to visualize the direct comparison. The SEC-DW results are in very good agreement with those from AUC-SV and Cryo-EM across the entire range (0–91% full capsids, or 0–98% empty), demonstrating that the SEC-DW results are reliable and accurate. Due to the presence of partial capsids in the samples used, the upper limit of the current SEC-DW method is approximately 91% full capsids, or 0% empty capsids.